Available online at www.pelagiaresearchlibrary.com

Pelagia Research Library

Advances in Applied Science Research, 2014, 5(3):114-129

ISSN: 0976-8610
CODEN (USA): AASRFC

Heat source/sink effects of heat and mass transfer of magneto-nanofluids over a nonlinear stretching sheet

Thommaandru Ranga Rao[1], Kotha Gangadhar[2], B. Hema Sundar Raju[3] and M. Venkata Subba Rao[3]

[1]*Department of Mathematics, SVKP College, Markapur, Prakasam, India*
[2]*Department of Mathematics, Acharya Nagarjuna University, Ongole, Andhra Pradesh, India*
[3]*Department of Mathematics, Vignan University, Guntur, Andhra Pradesh, India*

ABSTRACT

This study investigates theoretically the problem of free convection boundary layer flow of nanofluids over a non-linear stretching sheet in the presence of MHD and heat source/sink. The governing partial differential equations are transformed to a system of ordinary differential equations and solved numerically using fourth order Runge-Kutta method along with shooting technique. The effects of the magnetic parameter, the Prandtl number, Lewis number, power law velocity parameter, the Brownian motion parameter, thermophoresis parameter, heat source/sink parameter on the fluid properties as well as on the heat and mass transfer coefficients are determined and shown graphically.

Keywords: nanofluid, MHD, heat source/sink, Brownian motion, thermophoresis, nonlinear stretching sheet.

INTRODUCTION

The study of convective heat transfer in nanofluids is gaining a lot of attention. The nanofluids have many applications in the industry since materials of nanometer size have unique physical and chemical properties. Nanofluids are solid-liquid composite materials consisting of solid nanoparticles or nanofibers with sizes typically of 1-100 nm suspended in liquid. Nanofluids have attracted great interest recently because of reports of greatly enhanced thermal properties. For example, a small amount (<1% volume fraction) of Cu nanoparticles or carbon nanotubes dispersed in ethylene glycol or oil is reported to increase the inherently poor thermal conductivity of the liquid by 40% and 150%, respectively [1,2]. Conventional particle-liquid suspensions require high concentrations (>10%) of particles to achieve such enhancement. However, problems of rheology and stability are amplified at high concentrations, precluding the widespread use of conventional slurries as heat transfer fluids. In some cases, the observed enhancement in thermal conductivity of nanofluids is orders of magnitude larger than predicted by well-established theories. Other perplexing results in this rapidly evolving field include a surprisingly strong temperature dependence of the thermal conductivity [3] and a three-fold higher critical heat flux compared with the base fluids [4,5]. These enhanced thermal properties are not merely of academic interest. If confirmed and found consistent, they would make nanofluids promising for applications in thermal management. Furthermore, suspensions of metal nanoparticles are also being developed for other purposes, such as medical applications including cancer therapy. The interdisciplinary nature of nanofluid research presents a great opportunity for exploration and discovery at the frontiers of nanotechnology. Bachok et al. [6] studied boundary layer flow of a nanofluid past a moving plate in a uniform free stream. In another investigation, Bachok et al. [7] discussed heat transfer over a permeable stretching sheet for the unsteady boundary layer flow of a nanofluid. Kandasamy et al. [8] studied scaling group transformations for an electrically conducting nanofluid flow over a vertical stretching sheet. Tsou et al. [9] reported both analytical and experimental results for the flow and heat transfer in the boundary layer on a continuously

moving surface. Gorla et al. [10] studied the natural convective boundary layer flow over a horizontal plate embedded in a porous medium saturated with a nanofluid.

The magnetohydrodynamic (MHD) flow has attracted a great interest to many researchers during the last several decades owing to the effect of magnetic field on the boundary layer flow control and applications in many engineering and physical aspects such as MHD generators, plasma studies, nuclear reactors, geothermal energy extractions. Flow characteristics and heat transfer over a stretching sheet have been studied extensively by many researchers in the recent past because of many engineering applications of stretching sheet in manufacturing processes such as hot rolling, wire drawing, drawing of plastic films and artificial fibers, metal extrusion, crystal growing, continuous casting, glass fiber production and paper production. Metallurgy lies in the purification of molten metal's from non-metallic inclusions by applying magnetic field is other application of MHD. Chen [11] studied the effects of magnetic field and suction/injection on convection heat transfer of non-Newtonian power-law fluids past a power law stretched sheet with surface heat flux. The magnetohydrodynamic (MHD) forced convection boundary layer flow of nanofluid over a horizontal stretching plate was investigated by Nourazar et al. [12] using homotopy perturbation method (HPM). Matin et al. [13] studied entropy analysis in mixed convection MHD flow of nanofluid over a nonlinear stretching sheet. Hayat et al. [14] used homotopy analysis method (HAM) to investigate the MHD boundary layer flow and examine the heat transfer analysis for the permeable stretching sheet under varied conditions. In this continuation, Abbas and Hayat [15] studied the stagnation point flow with slip effects in heat transfer analysis for the boundary layer flow over a non-linear stretching sheet. Aman and Ishak [16] presented the hydromagnetic flow and heat transfer adjacent to a stretching vertical sheet with prescribed surface heat flux.

The boundary layer flows of non-Newtonian fluids over a stretching sheet with heat and mass transfer are important in several areas such as extrusion process, glass fibber, paper production, hot rolling, wire drawing, electronic chips, crystal growing, plastic manufactures, and application of paints, food processing and movement of biological fluids (Hayat and Qasim, [17]). Bhargava et al. [18] discussed heat and mass transfer of boundary layer flow over a non-linear stretching sheet under the effects of different physical parameters. Khan and Pop [19] investigated the laminar fluid flow of a nanofluid from the stretching flat surface by incorporating the effects of Brownian motion, thermophoresis and reported to be the pioneer for this study of stretching sheet in nanofluid. Pal and Mondal [20] examined the heat and mass transfer over a stretching sheet by considering the effects of buoyancy and solutal buoyancy parameters. Anwar et al. [21] studied the conjugate effects of heat and mass transfer of nanofluids over a nonlinear stretching sheet.

The heat source/sink effects in thermal convection, are significant where there may exist a high temperature differences between the surface (e.g. space craft body) and the ambient fluid. Heat generation is also important in the context of exothermic or endothermic chemical reactions. Vajravelu and Hadjinicalaou [22] have studied on hydrodynamic convective heat transfer from a stretching surface with heat generation/absorption. Molla et al. [23] studied natural convection flow along a vertical wavy surface with uniform surface temperature in presence of heat generation/absorption. MHD heat and mass transfer free convection flow along a vertical stretching sheet in presence of magnetic field with heat generation are studied by Samad et al. [24]. Recently, Rahman et al. [25] investigated the thermophoresis effect on MHD forced convection on a fluid over a continuous linear stretching sheet in presence of heat generation and Power-Law wall temperature

However, the interaction of conjugate effects of nanofluids over a nonlinear stretching sheet, has received little attention. Hence, the present study an attempt is made to analyze the steady conjugate effects of heat and mass transfer of nanofluid flow over a nonlinear stretching sheet in the presence of MHD and heat source/sink. The governing boundary layer equations have been transformed to a two-point boundary value problem in similarity variables and the resultant problem is solved numerically using the fourth order Runge-Kutta method along with shooting technique. The effects of various governing parameters on the fluid velocity, temperature, concentration, skin friction, reduced Nusselt number and reduced Sherwood number are shown in figures and analyzed in detail.

2. MATHEMATICAL FORMULATION

The steady two-dimensional boundary layer flow of a nanofluid past a stretching surface is considered under the assumptions that the external pressure on the plate in *x*-direction is having diluted nanoparticles. The stretching velocity is assumed to be $U_w(x) = U_0 x^m$, where U_0 is the uniform velocity and $m(m \geq 0)$ is a constant parameter and *x* is the coordinate measured along the stretching surface. The flow takes place above the stretching surface at $y \geq 0$. Here, *y* is the coordinate axis measured normal to the stretching surface. A uniform stress leading to equal and opposite forces is applied along the *x*-axis so that the sheet is stretched, keeping the origin fixed. A uniform magnetic field of strength *B*(x) is applied normal to the Sheet. It is assumed that at the stretching surface,

the temperature *T* and the nanoparticle fraction *C* take constant values T_w and C_w whereas the ambient values of temperature T_∞ and the nanoparticle fraction C_∞ are attained as *y* tends to infinity. Under these assumptions along with the Boussinesq and boundary layer approximations, the system of equations, governing the flow field are given by

Continuity equation

$$\frac{\partial u}{\partial x}+\frac{\partial v}{\partial y}=0 \tag{2.1}$$

Momentum equation

$$\frac{\partial p}{\partial x}=\mu\frac{\partial^2 u}{\partial y^2}-\rho_f\left(u\frac{\partial u}{\partial x}+v\frac{\partial u}{\partial y}\right)-\sigma B^2 u$$
$$+\left[\left(1-C_\infty\right)\rho_{f_\infty}\beta_T\left(T-T_\infty\right)-\left(\rho_f-\rho_{f_\infty}\right)\beta_C\left(C-C_\infty\right)\right]g \tag{2.2}$$

Energy equation

$$u\frac{\partial T}{\partial x}+v\frac{\partial T}{\partial y}=\alpha\nabla^2 T+\tau\left[D_B\frac{\partial\hat{\phi}}{\partial\hat{y}}\frac{\partial T}{\partial\hat{y}}+\frac{D_T}{T_\infty}\left(\frac{\partial T}{\partial y}\right)^2\right]+\frac{q}{\rho_f c_p}\left(T-T_\infty\right) \tag{2.3}$$

Species equation

$$u\frac{\partial C}{\partial x}+v\frac{\partial C}{\partial y}=D_B\frac{\partial^2 C}{\partial y^2}+\frac{D_T}{T_\infty}\frac{\partial^2 T}{\partial y^2} \tag{2.4}$$

The boundary conditions for the velocity, temperature and concentration fields are

$$u=U_w(x)=U_0x^m, v=0, T=T_w, C=C_w \quad \text{at} \quad y=0$$
$$u\to 0, v\to 0, T\to T_\infty, C\to C_\infty \quad \text{as} \quad \hat{y}\to\infty \tag{2.5}$$

where *u* and *v* are the velocity components along the *x* and *y* axes, respectively, g is the acceleration due to gravity, μ is the viscosity, ρ_f is the density of the base fluid, ρ_p is the density of the nanoparticle, β_T is the coefficient of the volumetric thermal expansion, β_C is the coefficient of the volumetric concentration expansion, $(\rho c)_f$ and $(\rho c)_p$ are the heat capacity of the fluid and the effective heat capacity of the nanoparticle material respectively, $\upsilon=\mu/\rho_f$ is the kinematic viscosity of the fluid, *k* is the thermal conductivity, $B(x)=B_0x^{\frac{m-1}{2}}$ is the magnetic field of constant strength, where B_0 is constant, $\alpha=k/(\rho c)_f$ is the thermal diffusivity parameter, D_B is the Brownian diffusion coefficient, τ is a parameter defined by $(\rho c)_f/(\rho c)_p$, $q=q_0x^{\frac{m-1}{2}}$ is the heat source/sink parameter, where q_0 is any constant.

The continuity equation (2.1) is satisfied by the Cauchy Riemann equations

$$u=\frac{\partial\psi}{\partial y} \quad \text{and} \quad v=-\frac{\partial\psi}{\partial x} \tag{2.6}$$

where $\psi(x,y)$ is the stream function.

In order to transform the equations (2.2) to (2.5) into a set of ordinary differential equations, the following similarity transformations and dimensionless variables are introduced.

$$\psi = \sqrt{\frac{2\upsilon U_0 x^{m+1}}{m+1}}, \eta = y\sqrt{\frac{(m+1)U_0 x^{m-1}}{2\upsilon}}, \theta(\eta) = \frac{T-T_\infty}{T_w - T_\infty}, \phi(\eta) = \frac{C-C_\infty}{C_w - C_\infty}$$
$$M = \frac{\sigma B_0^2}{\rho_f U_0}, \lambda = \frac{Gr}{\mathrm{Re}_x^{3/2}}, \delta = \frac{Gm}{\mathrm{Re}_x^{3/2}}, \mathrm{Pr} = \frac{\upsilon}{\alpha}, Le = \frac{\upsilon}{D_B}$$
$$Nb = \frac{\tau D_B (C_w - C_\infty)}{\upsilon}, Nt = \frac{\tau D_T (T_w - T_\infty)}{T_\infty \upsilon}, \mathrm{Re}_x = \frac{U_w(x)x}{\upsilon}, Q = \frac{q_0}{U_0 \rho_f c_p} \quad (2.7)$$
$$Gr = \frac{(1-C_\infty)\left(\frac{\rho_{f_\infty}}{\rho_f}\right) gn(T_w - T_\infty)}{\upsilon^2 \mathrm{Re}_x^{1/2}}, Gm = \frac{\left(\frac{\rho_p - \rho_{f_\infty}}{\rho_f}\right) gn_1(C_w - C_\infty)}{\upsilon^2 \mathrm{Re}_x^{1/2}}$$

where $f(\eta)$ is the dimensionless stream function, θ - the dimensionless temperature, ϕ - the nanoparticle volume friction, η - the similarity variable, Nb - the Brownian motion parameter, Nt - the thermophoresis parameter, *Pr* - the Prandtl number, Q- heat source/sink parameter, λ- thermal buoyancy parameter, δ-solutal buoyancy parameter, Re_x - the local Reynolds number based on the stretching velocity, M - the magnetic parameter, Le - the Lewis number, Gr-local thermal Grashof number, Gm-local solutal Grashof number. Here, β_T and β_C are proportional to x^{-3} , that is $\beta_T = nx^{-3}, \beta_C = n_1 x^{-3}$, where n and n_1 are the constant of proportionality (Makinde and Olenrewaju [26]).

In view of the equations (2.6) and (2.7), the equations (2.2) to (2.5)) transform into

$$f''' + ff'' - \frac{2m}{m+1} f'^2 + \frac{2}{m+1}(\lambda\theta - \delta\phi - Mf') = 0 \quad (2.8)$$

$$\frac{1}{\mathrm{Pr}}\theta'' + f\theta' + Nb\theta'\phi' + Nt\theta'^2 + \frac{2}{m+1}Q\theta = 0 \quad (2.9)$$

$$\phi'' + Lef\phi' + \frac{Nt}{Nb}\theta'' = 0 \quad (2.10)$$

The transformed boundary conditions can be written as

$$f = 0, f' = 1, \theta = 1, \phi = 1 \quad \text{at} \quad \eta = 0$$
$$f' \to 0, \theta \to 0, \phi \to 0 \quad \text{as} \quad \eta \to \infty \quad (2.11)$$

The skin-friction, Nusselt number and Sherwood number for the present problem of nanofluid are defined as

$$C_f = \frac{\tau_w}{\frac{1}{2}\rho U^2}, Nu = \frac{q_w x}{k(T_w - T_\infty)}, Sh = \frac{q_m x}{k(C_w - C_\infty)} \quad (2.12)$$

where

$$q_w = -k\frac{\partial T}{\partial y}, q_m = -D_B\frac{\partial C}{\partial y}, \tau_w = \mu\frac{\partial u}{\partial y} \quad \text{at } y=0$$

The associated expressions of dimensionless skin-friction $-f''(0)$, reduced Nusselt number $-\theta'(0)$ and reduced Sherwood number $-\phi'(0)$ defined as

$$Cfx = \frac{C_f}{2}\sqrt{\frac{2}{m+1}}\mathrm{Re}_x, Nu_r = \frac{Nu}{\sqrt{\frac{m+1}{2}\mathrm{Re}_x}}, Sh_r = \frac{Sh}{\sqrt{\frac{m+1}{2}\mathrm{Re}_x}} \tag{2.13}$$

3 SOLUTION OF THE PROBLEM

The set of non-linear coupled differential Eqs. (2.8)-(2.10) subject to the boundary conditions Eq. (2.11) constitute a two-point boundary value problem. In order to solve these equations numerically we follow most efficient numerical shooting technique with fifth-order Runge-Kutta-integration scheme. In this method it is most important to choose the appropriate finite values of $\eta \to \infty$. To select η_∞ we begin with some initial guess value and solve the problem with some particular set of parameters to obtain f'', θ' and ϕ'. The solution process is repeated with another large value of η_∞ until two successive values of f'', θ' and ϕ' differ only after desired digit signifying the limit of the boundary along η. The last value of η_∞ is chosen as appropriate value of the limit $\eta \to \infty$ for that particular set of parameters. The three ordinary differential Eqs. (2.8)-(2.10) were first formulated as a set of seven first-order simultaneous equations of seven unknowns following the method of superposition [27]. Thus, we set

,

$$y_1 = f, y_2 = f', y_3 = f'', y_4 = \theta, y_5 = \theta', y_6 = \phi, y_7 = \phi'$$

$$y_1' = y_2, y_2' = y_3$$

$$y_1(0) = 0, y_2(0) = 1$$

$$y_3' = \frac{2m}{m+1}y_2^2 + \frac{2}{m+1}(\delta y_6 + M y_2 - \lambda y_4) - y_1 y_3$$

$$y_3(0) = \delta_1$$

$$y_4' = y_5, y_4(0) = 1$$

$$y_5' = -\mathrm{Pr}\left[y_1 y_5 + Nb y_5 y_7 + Nt y_5^2 + \frac{2}{m+1}Q y_4\right]$$

$$y_5(0) = \delta_2$$

$$y_6' = y_7, y_6(0) = 1$$

$$y_7' = -\left[Le y_1 y_7 + \frac{Nt}{Nb}y_5'\right]$$

$$y_7(0) = \delta_3$$

Eqs. (2.8)-(2.11) then reduced into a system of ordinary differential equations, i.e., where δ_1, δ_2 and δ_3 are determined such that it satisfies $y_2(\infty) \to 0, y_4(\infty) \to 0$ and $y_6(\infty) \to 0$. The shooting method is used to guess δ_1, δ_2 and δ_3 until the boundary conditions $y_2(\infty) \to 0, y_4(\infty) \to 0$ and $y_6(\infty) \to 0$ are satisfied. Then the resulting differential equations can be integrated by fifth-order Runge-Kutta integration scheme. The above procedure is repeated until we get the results up to the desired degree of accuracy, 10^{-6}.

RESULTS AND DISCUSSION

In order to get a clear insight of the physical problem, the velocity, temperature and concentration have been discussed by assigning numerical values to the governing parameters encountered in the problem. Numerical computations are shown from figs.1-11.

The velocity for different values of the magnetic field parameter (*M)* is shown in fig.1. As is now well known, the velocity decreases with increases in the magnetic field parameter due to an increase in the Lorentz drag force that opposes the fluid motion. Figs. 2(a) to 2(c) are shows the effect of the thermal buoyancy parameter on the velocity, temperature and concentration profiles. The thermal buoyancy parameter signifies the relative effect of the thermal

buoyancy force to the viscous hydrodynamic force. The flow is accelerated due to the enhancement in buoyancy force corresponding to an increase in the thermal buoyancy parameter, i.e. free convection effects. It is noticed that the thermal buoyancy parameter influence the velocity field almost in the boundary layer when compared to far away from the plate. It is seen that as the thermal buoyancy parameter increases, the velocity field increases. Also noticed that temperature and concentration profiles decreases with an increasing the thermal buoyancy parameter. Figs. 3(a) to 3(c) are shows the effect of the solutal buoyancy parameter on the velocity, temperature and concentration profiles. It is seen that as the solutal buoyancy parameter increases, the velocity field decreases. Also observed that temperature and concentration profiles increases with an increasing the solutal buoyancy parameter.

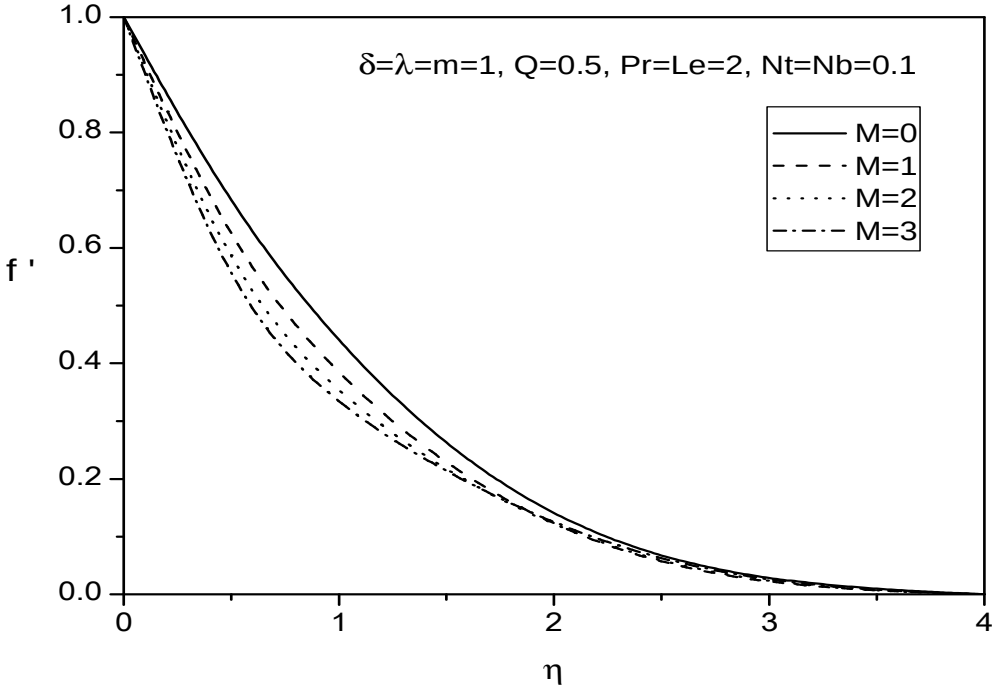

Fig.1 Velocity for different values of *M*

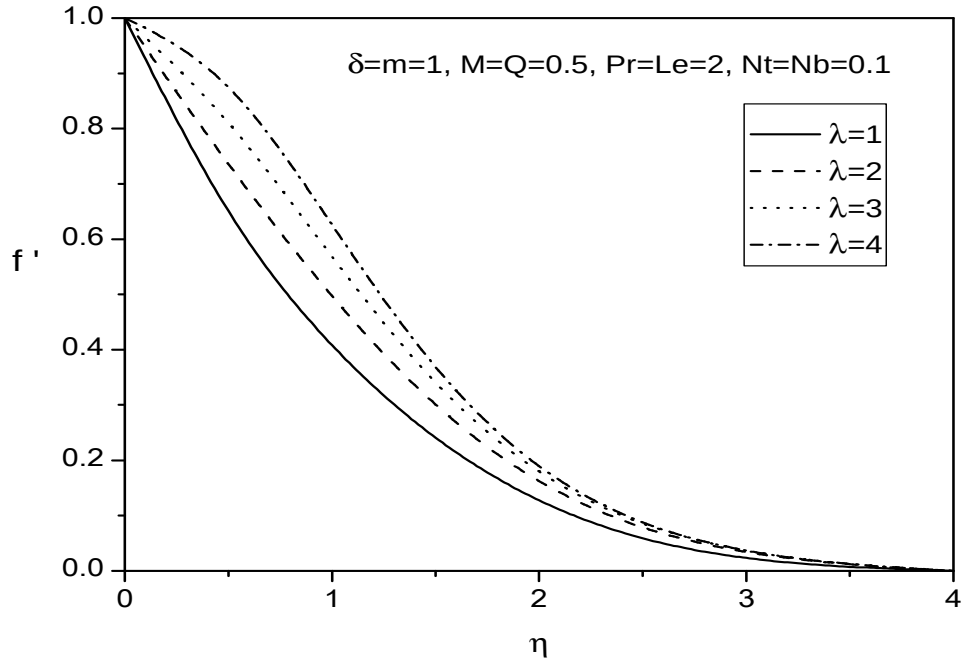

Fig.2(a) Velocity for different values of *λ*

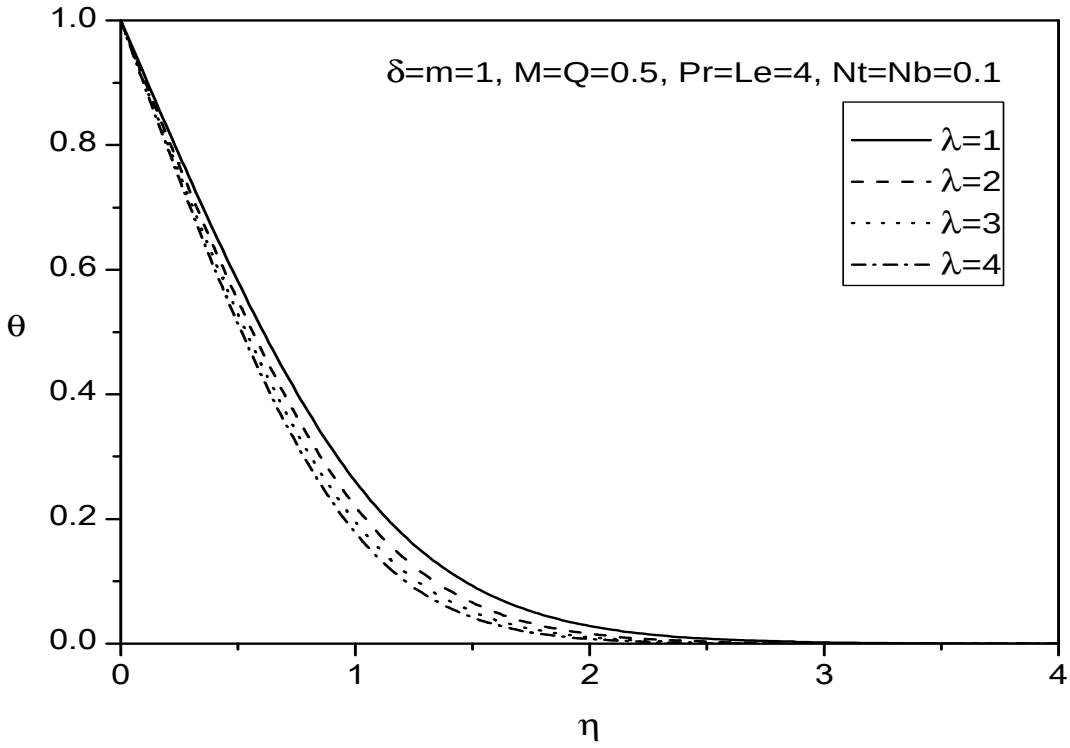

Fig.2(b) Temperature for different values of *λ*

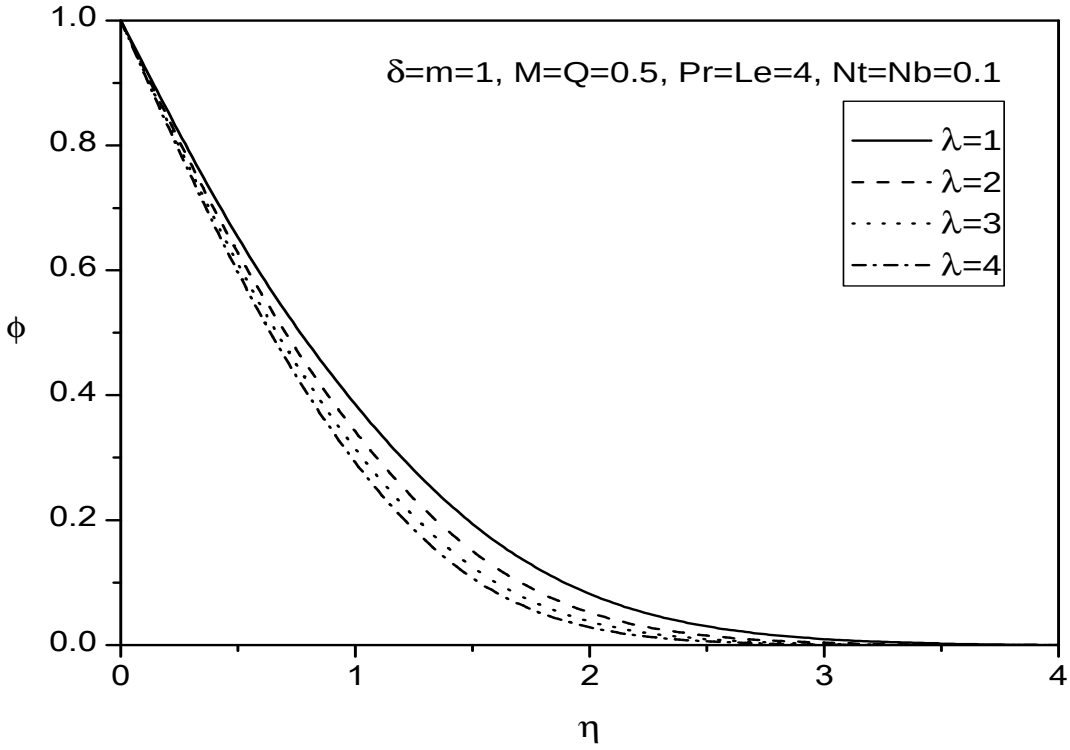

Fig.2(c) Concentration for different values of *λ*

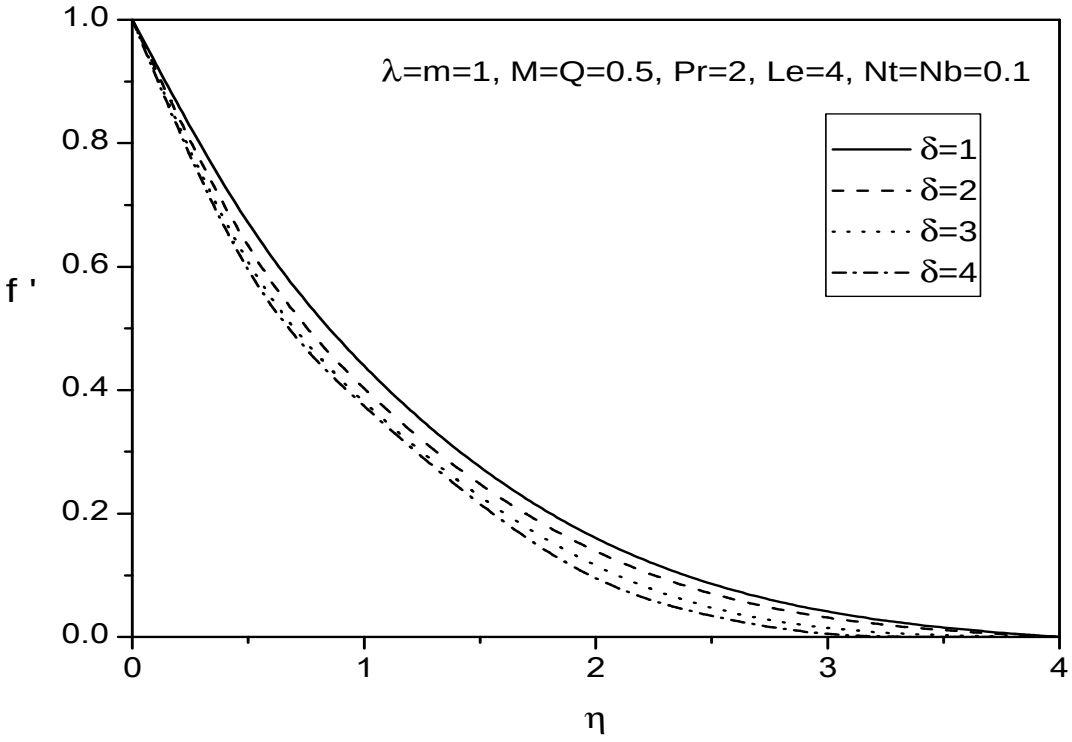

Fig.3(a) Velocity for different values of δ

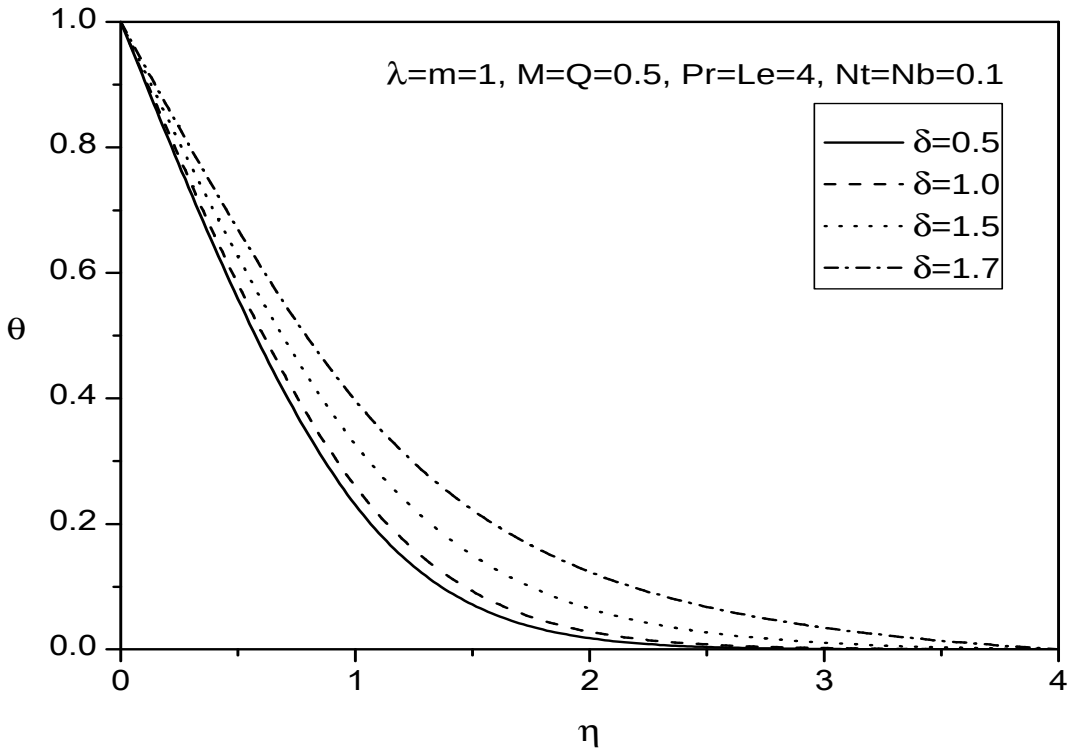

Fig.3(b) Temperature for different values of δ

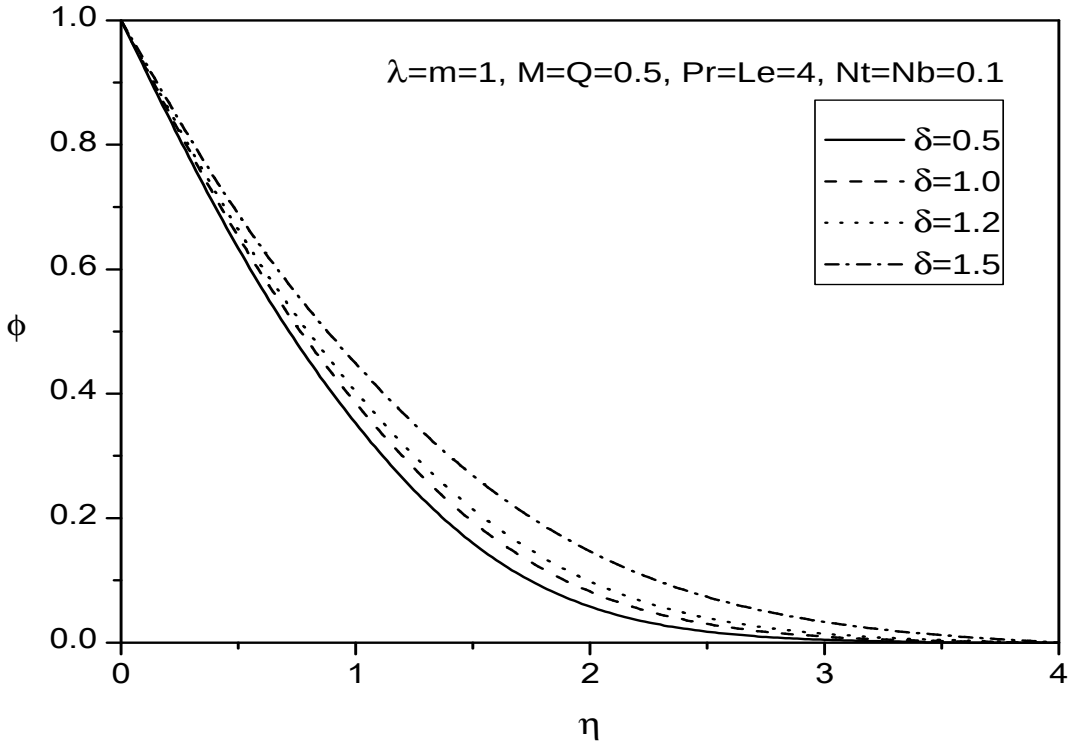

Fig.3(c) Concentration for different values of *δ*

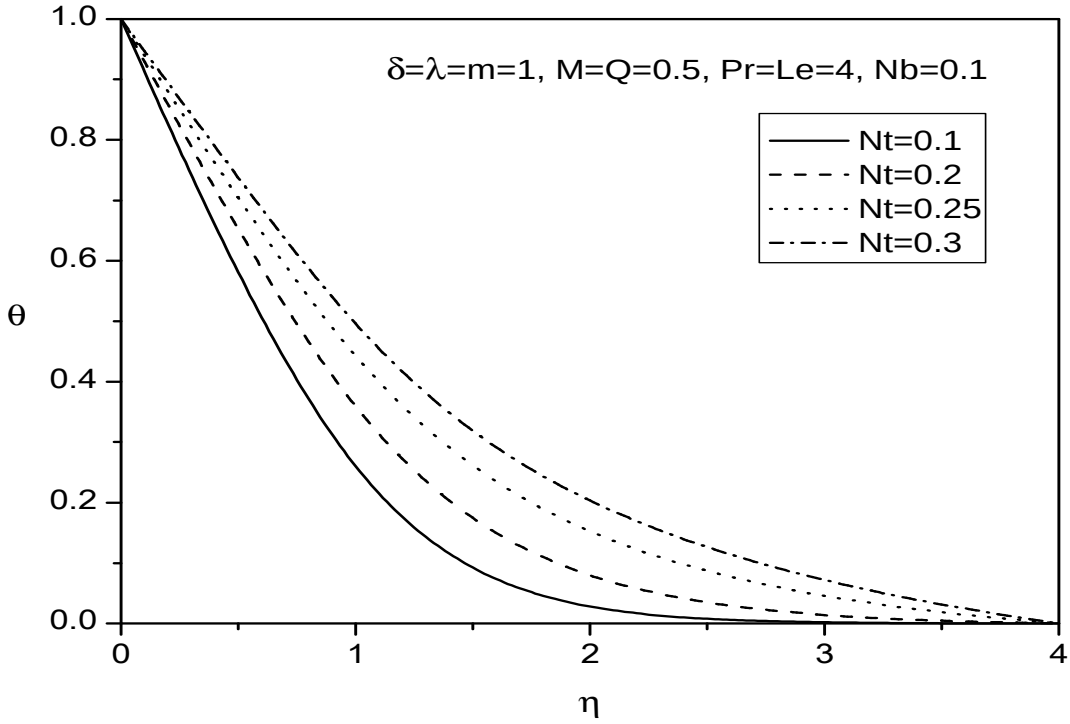

Fig.4(a) Temperature for different values of *Nt*

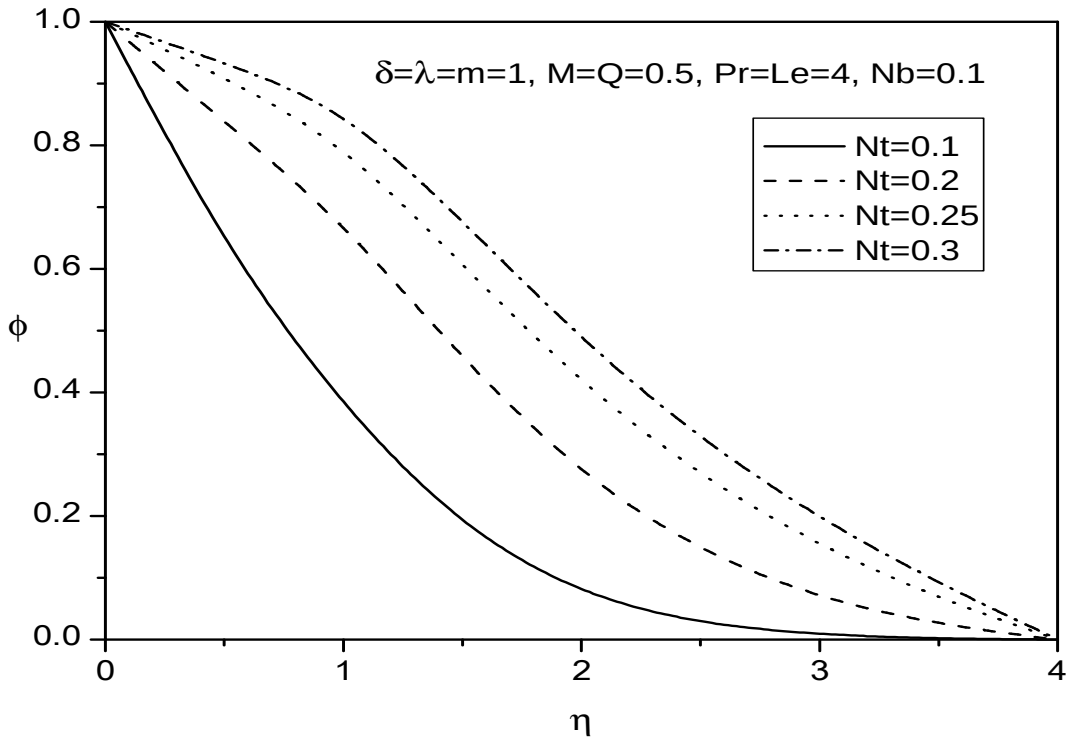

Fig.4(b) Concentration for different values of *Nt*

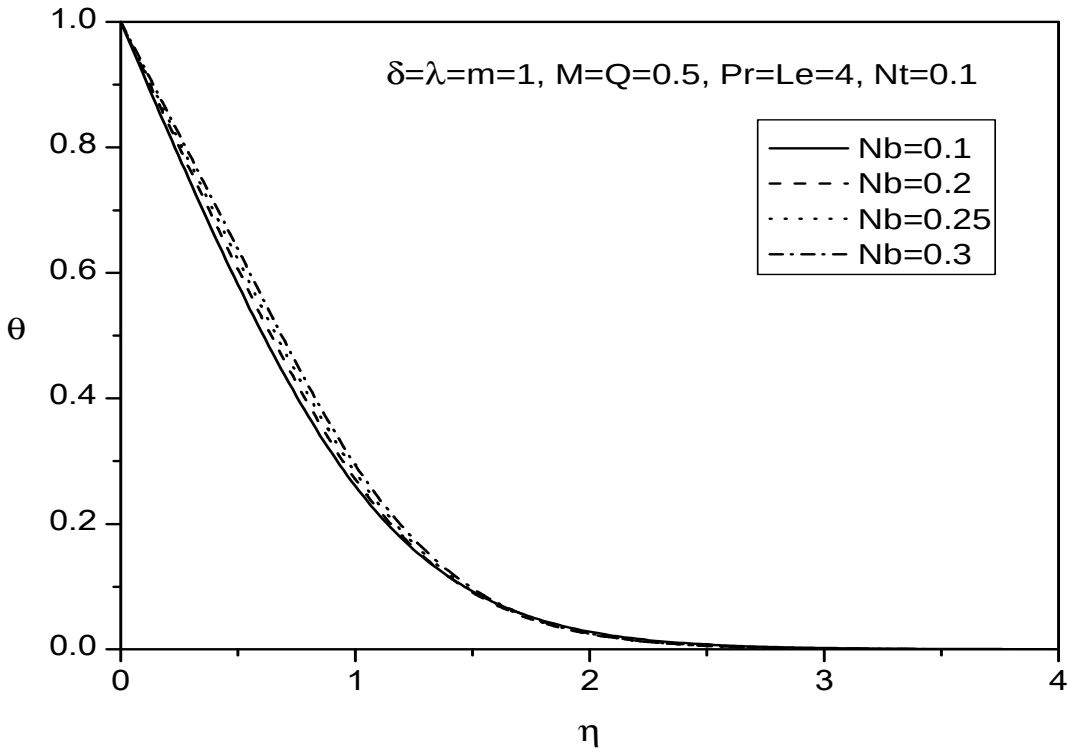

Fig.5(a) Temperature for different values of *Nb*

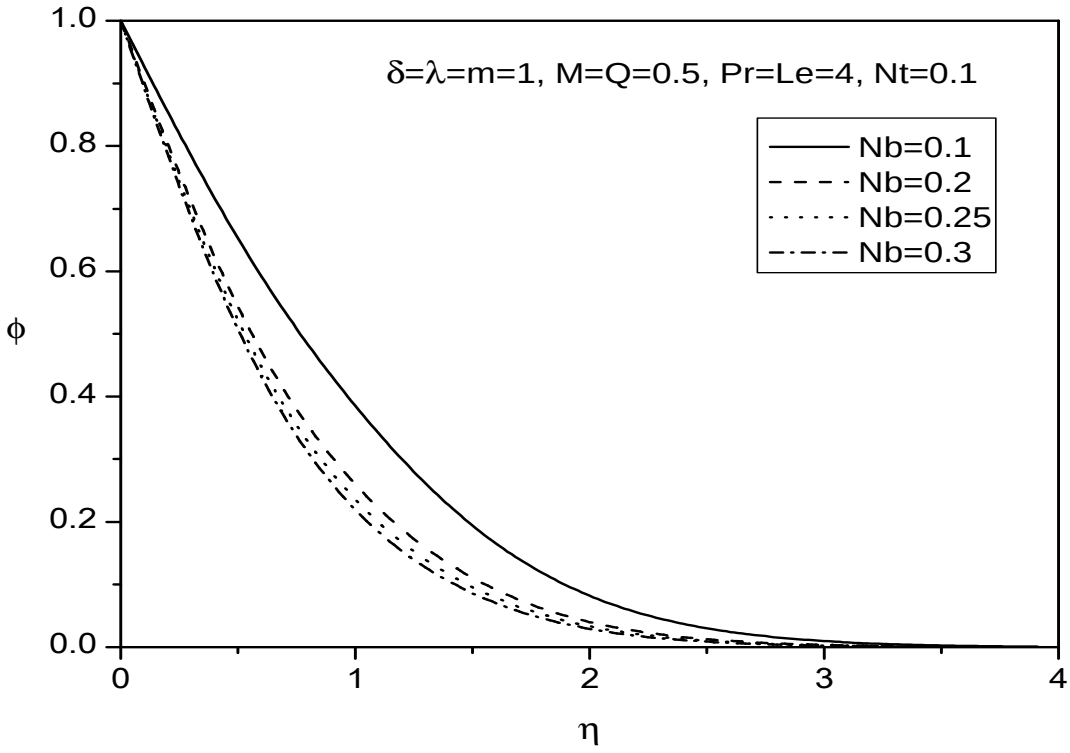

Fig.5(b) Concentration for different values of *Nb*

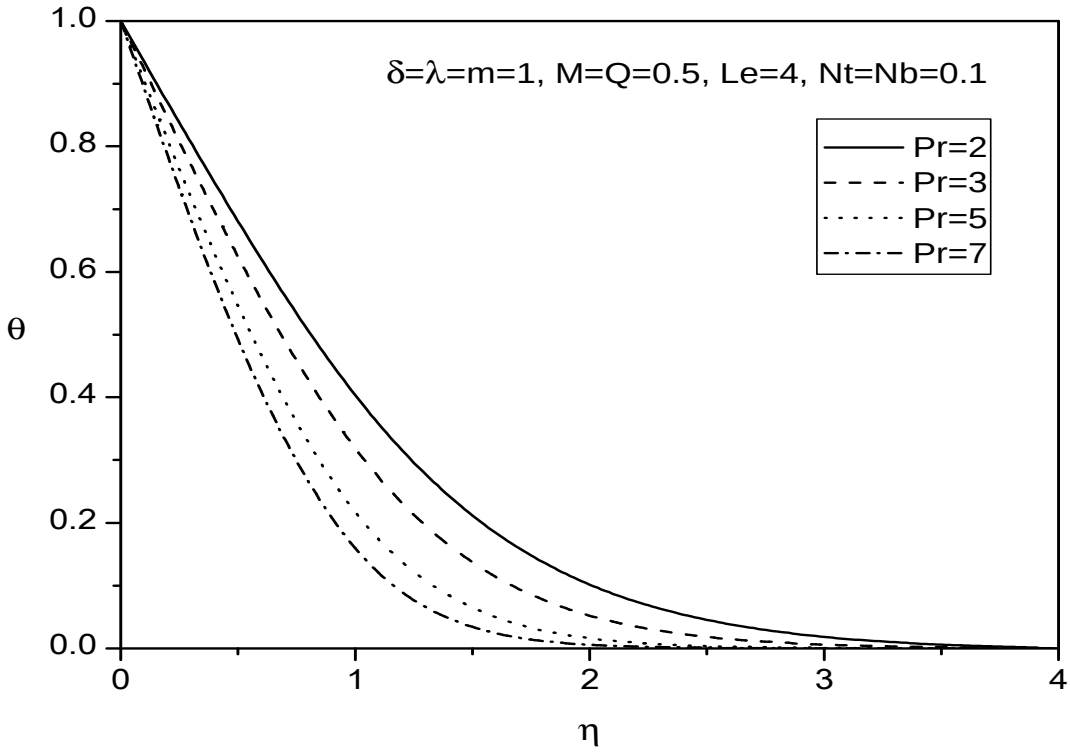

Fig.6 Temperature for different values of *Pr*

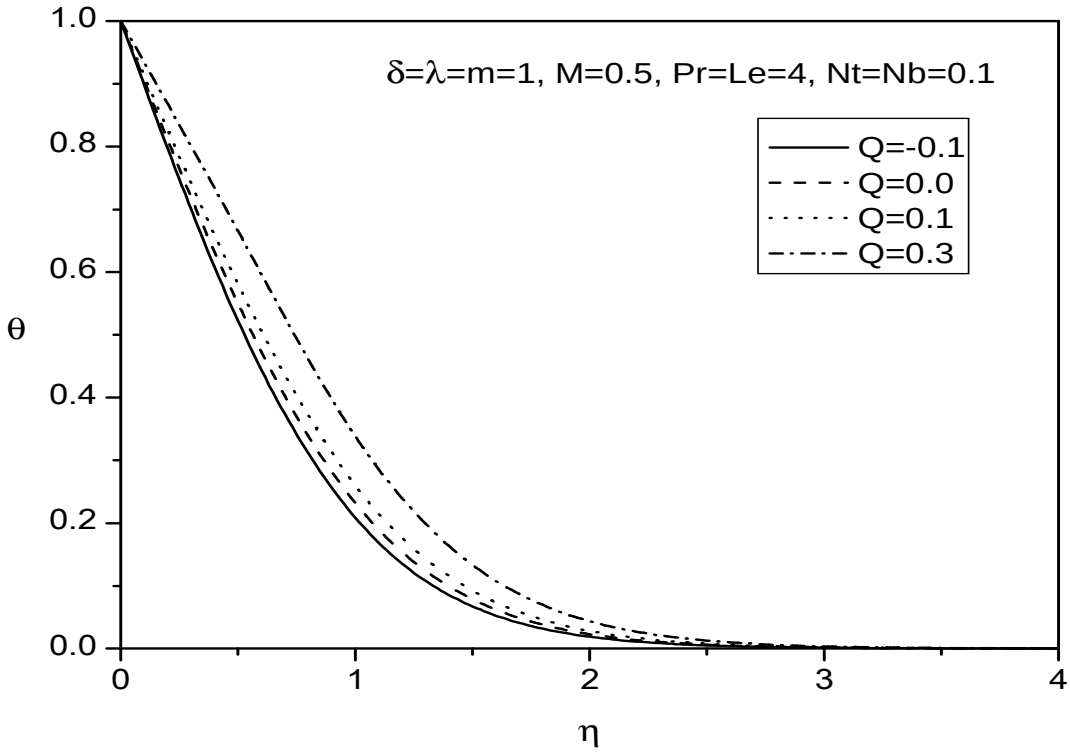

Fig.7 Temperature for different values of *Q*

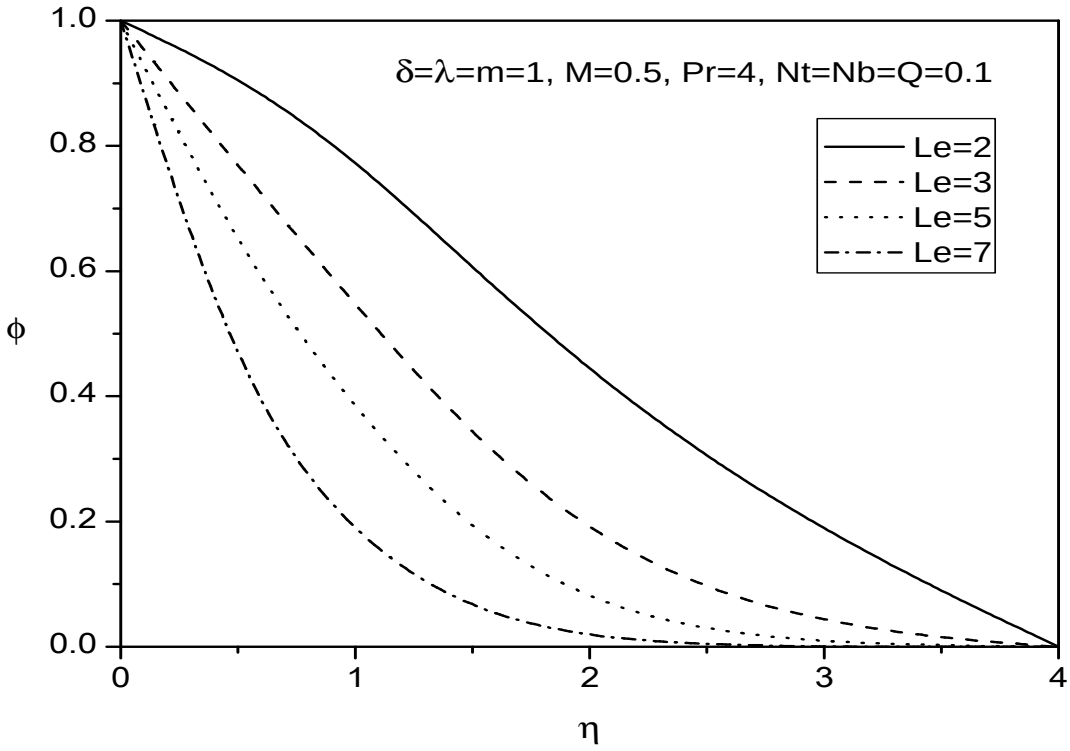

Fig.8 Concentration for different values of *Le*

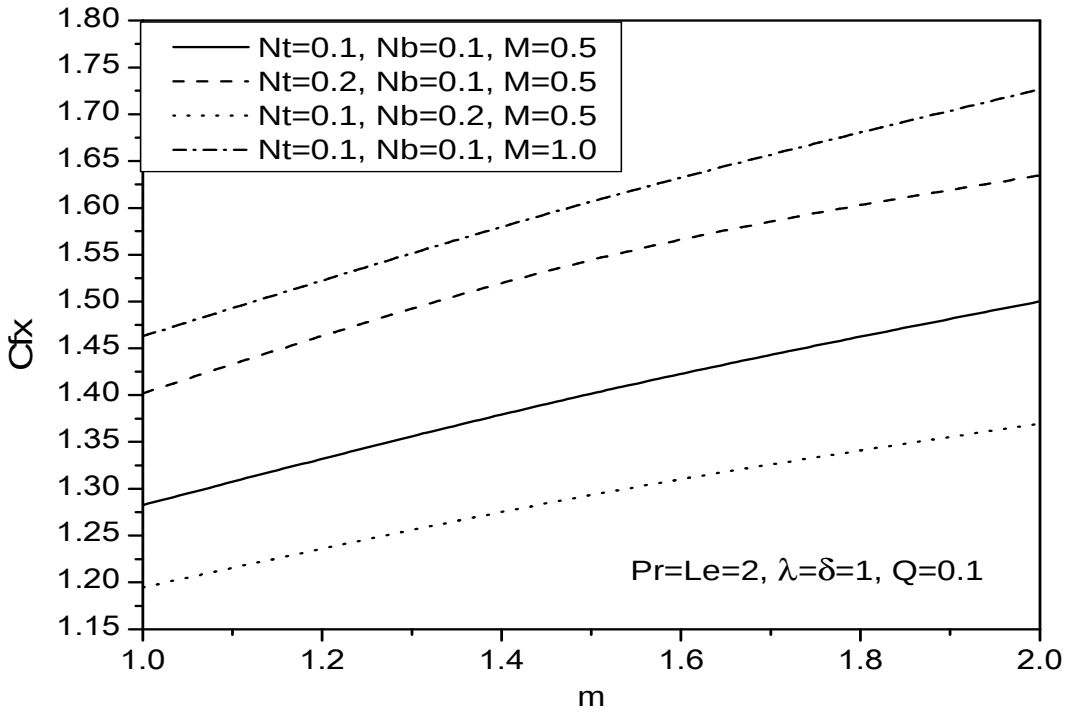

Fig.9 Effect of *Nt, Nb, Q* and *m* on the skin friction

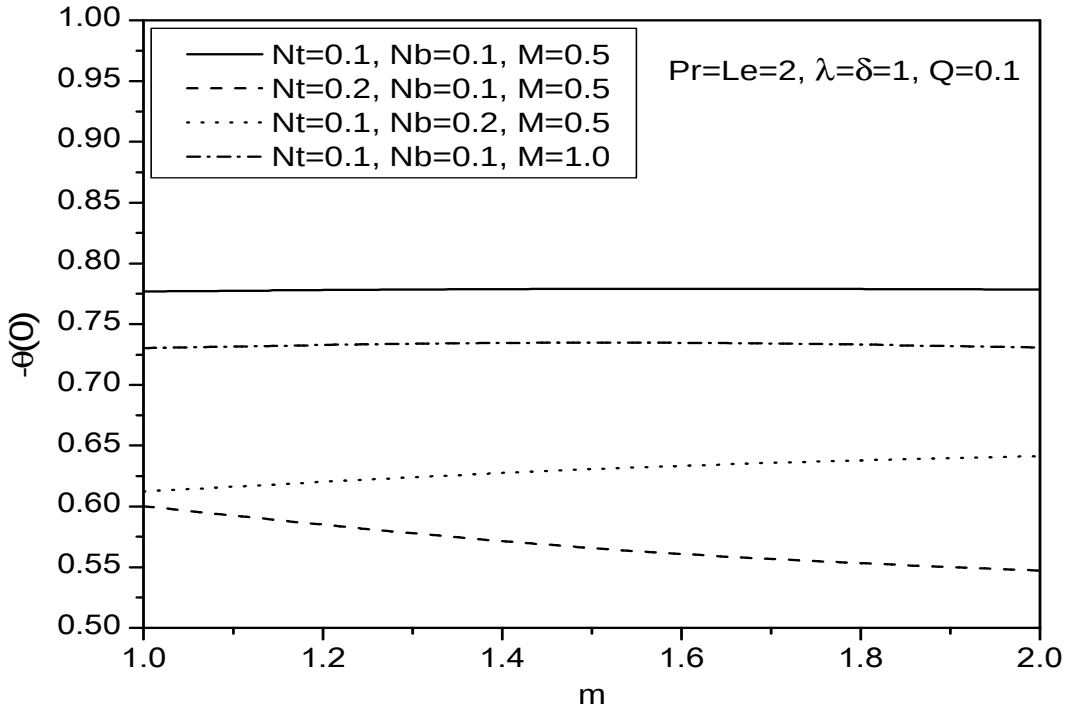

Fig.10 Effect of *Nt, Nb, Q* and *m* on the reduced Nusselt number

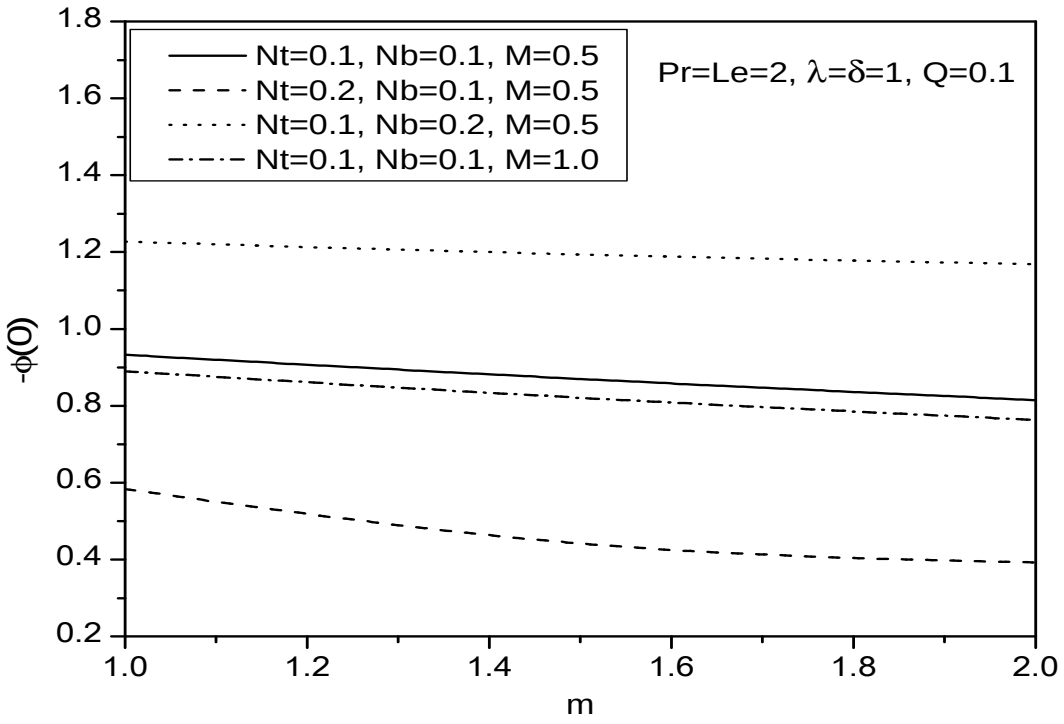

Fig.11 Effect of *Nt, Nb, Q* and *m* on the reduced Sherwood number

The effect of thermophoresis parameter on temperature and concentration fields is shown in figs. 4(a) and 4(b). The thermophoretic force generated by the temperature gradient creates a fast flow away from the stretching surface. In this way more fluid is heated away from the surface, and consequently, as *Nt* increases, the temperature within the boundary layer increases. The fast flow from the stretching sheet carries with it thermophoretic force leading to an increase in the concentration boundary layer thickness. The effect of the Brownian motion of the fluid on the temperature and concentration is shown in Figs. 5(a) and 5(b). As expected, the increased Brownian motion of the fluid carries with it heat and the thickness of the thermal boundary layer increases. An increase in the Brownian motion of the fluid leads to a decrease in the concentration profiles. Fig. 6 show the temperature profiles for several values of the Prandtl number (*Pr)*. The temperature profiles decrease as the Prandtl number increases since, for high Prandtl numbers, the flow is governed by momentum and viscous diffusion rather than thermal diffusion. Fig. 7 shows the effect of the heat source/sink parameter (*Q*) on the temperature profiles. The temperature profiles significantly increase as the heat source/sink parameter increases. The various values of Lewis number (*Le*) on concentration is plotted in fig. 8. The concentration profiles significantly contract as the Lewis number increases.

Fig. 9 shows the effects of the thermophoresis parameter, Brownian motion parameter, non linear stretching parameter (*m*) and the magnetic parameter on the wall skin friction. It can be seen that the skin friction coefficient increases when the thermophoresis parameter, non linear stretching parameter and magnetic parameter increases. However, increasing the Brownian motion parameter leads to a decrease in the skin friction coefficient. Figs. 10 show the effects of the thermophoresis parameter, Brownian motion parameter, non linear stretching parameter and the magnetic parameter on the reduced Nusselt number. We note a decrease in the reduced Nusselt number when *Nt or Nb or m or M* increases. Fig. 11 depicts the effects of the thermophoresis parameter, Brownian motion parameter, non linear stretching parameter and the magnetic parameter on the reduced Sherwood number $-\phi'(0)$. We observe an increase in the $-\phi'(0)$ when *Nb* increases and decrease when *Nt* or *m* or *M* increases.

The variations of skin friction coefficient, reduced Nusselt number and reduced Sherwood number for different values of λ, δ, *Pr*, *Q* and *Le* are shown in Table 2. It is observed that *Cfx* is an increasing function of δ and *Pr*, while with increasing values of λ, *Q* and *Le*. However, it is found that $-\theta'(0)$ decreases for large values of δ and *Q* whereas increases for increasing values of λ, *Pr* and *Le*. It is further observed from this table that $-\phi'(0)$ is increasing function of λ, δ, *Q* and *Le* whereas $-\phi'(0)$ decreases with increasing values of Pr. Table.1 shows the comparison of reduced Nusselt number and reduced Sherwood number of the previous published data.

Table 1 Comparison of reduced Nusselt number and reduced Sherwood number for Pr=10, Le=10, m=1, δ=λ=M=Q=0

Nt	*Nb*	Present study		Khan and Pop	
		$-\theta'(0)$	$-\phi'(0)$	$-\theta'(0)$	$-\phi'(0)$
0.1	0.1	0.952377	2.12939	0.9524	2.1294
0.2	0.2	0.365358	2.51522	0.3654	2.5152
0.3	0.3	0.135514	2.60882	0.1355	2.6088
0.4	0.4	0.0494649	2.60384	0.0495	2.6038
0.5	0.5	0.0179222	2.5731	0.0179	2.5731

Table 2: Variation of Cfx, $-\theta'(0)$ & $-\phi'(0)$ at the wall with Nb, Nt, Pr, Le, *λ, δ, m, Q* and *M*

Nb	*Nt*	*Pr*	*Le*	*λ*	*δ*	*m*	*Q*	*M*	Cfx	$-\theta'(0)$	$-\phi'(0)$
0.1	0.1	0.71	10	1	1	1	0.1	0.5	0.884488	0.398492	2.27777
0.5	0.1	0.71	10	1	1	1	0.1	0.5	0.859086	0.310482	2.35659
0.1	0.5	0.71	10	1	1	1	0.1	0.5	0.926766	0.333145	2.09201
0.1	0.1	5.0	10	1	1	1	0.1	0.5	1.14315	0.768753	2.11431
0.1	0.1	0.71	25	1	1	1	0.1	0.5	0.812171	0.403223	3.78752
0.1	0.1	0.71	10	3.5	1	1	0.1	0.5	-0.240852	0.51267	2.45858
0.1	0.1	0.71	10	1	1.5	1	0.1	0.5	0.995372	0.392782	2.26363
0.1	0.1	0.71	10	1	1	1.5	0.1	0.5	0.967224	0.400474	2.25289
0.1	0.1	0.71	10	1	1	1	0.3	0.5	0.826524	0.239725	2.37391
0.1	0.1	0.71	10	1	1	1	0.1	1.0	1.10094	0.368621	2.23811

CONCLUSION

In the present numerical study, conjugate effects of heat and mass transfer of nanofluids over a nonlinear stretching sheet in the presence of MHD and heat generation or absorption. We determined the effects of various parameters on the fluid properties as well as on the shin friction, heat and mass transfer rates. We have shown that increasing the magnetic field parameter *M* tends to retard the fluid flow within the boundary layer. The effects of the Prandtl number, the Lewis number, the Brownian motion parameter, the thermophoresis parameter, heat source/sink parameter on the skin friction, heat and mass transfer coefficients and fluid flow characteristics have been studied. We have observed that:

- The fluid velocity decreases when increasing the magnetic parameter.
- The thermal and mass boundary layer thickness increases with the thermophoresis parameter.
- Increasing the Lewis number and solutal buoyancy parameter reduces the heat and mass transfer coefficient.
- Increasing the Brownian motion parameter and heat source/sink parameters enhances the thermal boundary layer thickness.
- Non linear stretching parameter enhances the shin-friction.

REFERENCES

[1] Eastman, J. A., Choi, S. U. S., Yu, S. Li, W., and Thompson, L. J., (**2001**), *Applied Physics Letters*, Vol. 78, No. 6, pp. 718-720.
[2] Choi, S. U. S., Zhang, Z. G., Lockwood, W. Yu, F. E., and Grulke, E. A., (**2001**), *Applied Physics Letters*, Vol. 79, No. 14, pp. 2252-2254.
[3] Patel, H. E., Das, S. K., Sundararajan, T., Sreekumaran, A., George, B., and Pradeep, T., (**2003**), *Applied Physics Letters*, Vol. 14, No. 83, pp. 2931-2933.
[4] You, S. M., Kim, J. H., and Kim, K. H., (**2003**), *Applied Physics Letters*, Vol. 83, No. 16, pp. 3374-3376.
[5] Vassallo, P., Kumar, R., and D'Amico, S., (**2004**), *International Journal of Heat and Mass Transfer*, Vol. 47, No. 2, pp. 407-411.
[6] Bachok, N., Ishak, A., Pop, I., (**2010**), *Int. J. Therm. Sci.,* Vol.49, pp.1663-1668.
[7] Bachok, N., Ishak, A., and Pop, I., (**2012**), *Int. J. Heat Mass Transf*., Vol.55, pp.2102-2109.
[8] Kandasamy, R., Loganathan, P., Arasu, P.P., (**2011**), *Nucl. Eng. Des.*, Vol.241, pp.2053-2059.
[9] Tsou, F.K., Sparrow, E.M., and Goldstien, R.J., (**1967**), *Int. Heat Mass Trans., Vol.*10, pp.219-223.
[10] Rama Subba Reddy Gorla, and Ali Chamkha, (**2011**), *Journal of Modern Physics*, Vol. 2, pp.62-71.
[11] Chen, C.H., (**2008**), *Int. J. Thermal Sci*., Vol.47, pp.954-961.
[12] Nourazar, S.S., Matin, M.H., and Simiari, M., (**2011**), *J. Appl. Math.*, doi:10.1155/2011/876437.
[13] Matin, M.H., Heirani, M.R., Nobari, Jahangiri, P., (**2012**), *J. Therm. Sci. Technol*., Vol.7, pp.104-119.
[14] Hayat, T., Qasim, M., Mesloub, S., (**2011**), *Int. J. Numer. Methods Fluids*, Vol.66, pp.963-975.
[15] Abbas, Z., and Hayat, T., (**2011**), *Numer. Meth. Part Differ. Equat*., Vol.27, pp.302- 314.

[16] Aman, F., and Ishak, A., (**2010**), *Heat Mass Transf*., Vol.46, pp.615--620.
[17] Hayat, T.,and Qasim, M., (**2011**), *Int. J. Numer. Meth. Fluids*, Vol.66, pp.820-832.
[18] Bhargava, R., Sharma, S., Takhar, H.S., Beg, O.A., and Bhargava, P., (**2007**), *Nonlinear Anal. Model. Cont*., Vol.12, pp.45-63.
[19] Khan, W.A., and Pop, I., (**2010**), *Int. J. Heat Mass Transf*., Vol.53, pp.2477-2483.
[20] Pal, D., and Mondal, H., (20**1**0), *Physica* B., Vol.85, pp.941-951.
[21] Anwar, M. I., Khan, I., Sharidan, S., and Salleh, M. Z., (**2012**), *International Journal of Physical Sciences*, Vol. 7(26), pp. 4081 – 4092.
[22] Vajravelu, K., and Hadjinicolaou, A., (**1993**), *Int. Comm. Heat Mass Trans.*, Vol.20, pp.417-430.
[23] Molla, M.M., Hossain, M.A., and Yao, L.S., (**2004**), *Int. J. Thermal Sci.*, Vol.43, pp.157-163.
[24] Samad, M.A., and Mohebujjaman, M., (**2009**), *Research J. of Applied Sci., Eng. and Tech.*, Vol.1(3), pp.98-106.
[25] Mohammed Abdur Rahman, Alim, M. A. and Jahurul Islam, Md., (**2013**), *Annals of Pure and Applied Mathematics, Vol. 4, No.2, pp.192-204*
[26] Makinde, O.D., and Olanrewaju, P.O., (**2010**), *J. Fluids Eng. Trans*., ASME 132:044502-1-4.
[27] Na, T.Y., (**1979**), Computational Methods in Engineering Boundary Value Problems, Academic Press, New York.